2010-04

Kinetic mechanism and catalysis of Trypanossoma cruzi dihydroorotate dehydrogenase enzyme evaluated by isothermal titration calorimetry

Analytical Biochemistry,Maryland Heights : Academic Press,v. 399, n. 1, p. 13-22, Apr. 2010
http://www.producao.usp.br/handle/BDPI/50079

Analytical Biochemistry 399 (2010) 13–22

Contents lists available at ScienceDirect

Analytical Biochemistry

journal homepage: www.elsevier.com/locate/yabio

Kinetic mechanism and catalysis of *Trypanosoma cruzi* dihydroorotate dehydrogenase enzyme evaluated by isothermal titration calorimetry

Juliana Cheleski [a], Helton José Wiggers [b], Ana Paula Citadini [c], Antônio José da Costa Filho [c], Maria Cristina Nonato [d], Carlos Alberto Montanari [a,b,*]

[a] *Grupo de Química Medicinal de Produtos Naturais, NEQUIMED–PN, Departamento de Química e Física Molecular, Instituto de Química de São Carlos, Universidade de São Paulo, 13560-970 São Carlos, SP, Brazil*
[b] *Departamento de Química, Universidade Federal de São Carlos, 13565-905 São Carlos, SP, Brazil*
[c] *Grupo de Biofísica Molecular Sérgio Mascarenhas, Instituto de Física de São Carlos, Universidade de São Paulo, 13560-970 São Carlos, SP, Brazil*
[d] *Laboratório de Cristalografia de Proteínas, Faculdade de Ciências Farmacêuticas de Ribeirão Preto, Universidade de São Paulo, 14040-903 Ribeirão Preto, SP, Brazil*

ARTICLE INFO

Article history:
Received 31 August 2009
Received in revised form 14 November 2009
Accepted 15 November 2009
Available online 20 November 2009

Keywords:
Chagas disease
Trypanosoma cruzi
Dihydroorotate dehydrogenase
Enzyme kinetics
Activation thermodynamic parameters

ABSTRACT

Trypanosoma cruzi dihydroorotate dehydrogenase (TcDHODH) catalyzes the oxidation of L-dihydroorotate to orotate with concomitant reduction of fumarate to succinate in the *de novo* pyrimidine biosynthetic pathway. Based on the important need to characterize catalytic mechanism of TcDHODH, we have tailored a protocol to measure TcDHODH kinetic parameters based on isothermal titration calorimetry. Enzymatic assays lead to Michaelis–Menten curves that enable the Michaelis constant (K_M) and maximum velocity (V_{max}) for both of the TcDHODH substrates: dihydroorotate ($K_M = 8.6 \pm 2.6$ μM and $V_{max} = 4.1 \pm 0.7$ μM s^{-1}) and fumarate ($K_M = 120 \pm 9$ μM and $V_{max} = 6.71 \pm 0.15$ μM s^{-1}). TcDHODH activity was investigated using dimethyl sulfoxide (10%, v/v) and Triton X-100 (0.5%, v/v), which seem to facilitate the substrate binding process with a small decrease in K_M. Arrhenius plot analysis allowed the determination of thermodynamic parameters of activation for substrates and gave some insights into the enzyme mechanism. Activation entropy was the main contributor to the Gibbs free energy in the formation of the transition state. A factor that might contribute to the unfavorable entropy is the hindered access of substrates to the TcDHODH active site where a loop at its entrance regulates the open–close channel for substrate access.

Chagas disease or American trypanosomiasis, caused by the flagellate protozoan parasite *Trypanosoma cruzi,* has been considered one of the most neglected diseases in the world. The available control strategy has not fully helped to reduce disease burden. Despite Brazil's efforts to control this disease, a large segment of the population still suffers from its effects [1]. The most recent estimate data from the Disease Control Priorities Project of the National Institutes of Health and World Bank indicate an overall number of 9.8 million people infected with *T. cruzi* [2].

The progression of this disease can lead to symptoms such as inflammatory cardiomyopathy, neural disorders, and digestive injuries. A large percentage of Chagas patients receive no specific antiparasitic therapy because of the ineffectiveness and toxicity of the pharmacological agents in use (nifurtimox and benznidazole). Hence, better therapeutic agents and novel drug targets need to be developed, but when focusing on the challenges facing drug target selection and characterization, care must be taken before the search for active compounds can begin. This means that we must, for instance, describe the biochemical mechanism of targets to achieve active site complementarity (steric, electrostatic, and hydrophobic).

Trypanosoma cruzi dihydroorotate dehydrogenase (TcDHODH,[1] EC 1.3.99.11) catalyzes a coupled redox reaction in which dihydroorotate (DHO) is oxidized to orotate and fumarate is reduced to succinate. This is the fourth enzymatic step in the pyrimidine de novo biosynthetic pathway [3]. Although the enzymatic function of dihydroorotate dehydrogenases (DHODs) is conserved in all organisms, the enzymes in prokaryotic and eukaryotic organisms are quite different [4].

Based on amino acid sequence identity, DHODs have been classified into two families referred to as family 1 and family 2. Family

* Corresponding author. Address: Grupo de Química Medicinal de Produtos Naturais, NEQUIMED–PN, Departamento de Química e Física Molecular, Instituto de Química de São Carlos, Universidade de São Paulo, 13560-970 São Carlos, SP, Brazil. Fax: +55 16 3373 9985.
E-mail address: montana@iqsc.usp.br (C.A. Montanari).

[1] *Abbreviations used:* TcDHODH, *Trypanosoma cruzi* dihydroorotate dehydrogenase; DHO, dihydroorotate; DHOD, dihydroorotate dehydrogenase; NAD^+, nicotinamide adenine dinucleotide; ITC, isothermal titration calorimetry; DMSO, dimethyl sulfoxide; IPTG, isopropyl β-D-thiogalactoside; Ni–NTA, nickel–nitrilotriacetic acid; SDS–PAGE, sodium dodecyl sulfate–polyacrylamide gel electrophoresis; UV, ultraviolet; HTS, high-throughput screening; FMN, flavin mononucleotide.

0003-2697/$ - see front matter © 2009 Elsevier Inc. All rights reserved.
doi:10.1016/j.ab.2009.11.018

1 DHODs are cytoplasmic enzymes further subdivided into families 1A and 1B. The TcDHODH belongs to the 1A homodimer enzymes family that has fumarate as the reduced substrate, whereas the 1B enzymes are heterotetramers that use nicotinamide adenine dinucleotide (NAD^+) as an oxidizing agent. Family 2 DHODs are membrane-anchored enzymes that exist as monomers and use quinones as oxidizing agents [5].

Several antitumor and immunosuppressive drugs act on human DHOD. The two most promising drugs are brequinar (antitumor and immunosuppressive) and leflunomide (immunosuppressive). The latter has been Food and Drug Administration approved for use in rheumatoid arthritis (Arava, Hoechst Marion Roussel). The inhibition of DHODs causes a lowering of the intracellular pools of the nucleotide bases uracil, cytosine, and thymine, making DHODs attractive drug targets. In DHOD knockout studies, *T. cruzi* did not express the enzyme protein and could not survive even in the presence of pyrimidine nucleosides, confirming its dependence on de novo biosynthesis [6]. Because TcDHODH is a valid target, it is of the utmost importance to elucidate its catalytic mechanism and characterize its activity [7], thereby enabling the development of a rapid and sensitive method to measure the inhibitory activity of compounds.

Isothermal titration calorimetry (ITC) has been used in enzyme kinetic assays to elucidate enzyme catalytic mechanisms and determine Michaelis–Menten kinetic parameters [8]. The overall principle of ITC is the measurement of heat flow at constant temperature. The rate at which heat is produced or absorbed can be related to the rate of conversion taking place in an enzymatic reaction. The enzyme activity is monitored in real time without the need for any probe [9]. Although ITC is used to study thermodynamic properties of biological systems, this technique has not been explored in depth as a means of investigating enzyme inhibition. ITC has an advantage over commonly used assay methods due to its ability to detect heat changes during enzymatic conversion under conditions such as poor transparency of solution with no need for any chromogenic, fluorogenic, or radioisotope-enriched (labeled) ligands. Heat changes are fundamental during binding events as well as biochemical reactions; thus, ITC is an ideal method for the characterization of enzyme reactions [10].

In this article, we describe for the first time the determination of TcDHODH enzyme kinetic parameters by ITC. We also measure the inhibition constant and elucidate the mechanism of action of the reaction product, orotate, to establish a response pattern of TcDHODH when used to screen chemical substances. In addition, kinetic experiments were carried out in the presence of the cosolvent dimethyl sulfoxide (DMSO) [11], a common solvent that enhanced the solubility of chemical compounds in water, and Triton X-100, a nonionic surfactant used to prevent molecular aggregation that frequently leads to false positives during screening assays. It is also important to measure the free energy, enthalpy, and entropy of activation ($\Delta G^{\#}$, $\Delta H^{\#}$, and $\Delta S^{\#}$, respectively) of the enzymatic reaction to disclose the relative importance of the enthalpic and entropic contributions of substrate to catalysis. A description of the enzymatic transition state can be helpful in the design of transition state analogs and in the search for inhibitors with high affinity for the enzyme TcDHODH.

Materials and methods

Materials

Reagents required for cloning, expression, and purification of TcDHODH

Isopropyl β-D-thiogalactoside (IPTG) was obtained from Invitrogen Life Technologies (São Paulo, Brazil). Nickel–nitrilotriacetic acid (Ni–NTA) affinity resin was obtained from Qiagen (Hilden, Germany), and kanamycin antibiotic was obtained from Calbiochem (La Jolla, CA, USA). Protein standards used as sodium dodecyl sulfate–polyacrylamide gel electrophoresis (SDS–PAGE) markers were obtained from Sigma Chemical (St. Louis, MO, USA).

Chemical reagents required for enzyme kinetic assay

DHO, orotic acid (orotate), fumaric acid (fumarate), Trizma base, and dibasic and monobasic sodium phosphate were purchased from Sigma–Aldrich. Sodium chloride was obtained from Fluka.

Enzyme preparation

Recombinant TcDHODH was expressed and purified as described elsewhere [12]. Briefly, the purification of the yellow enzyme TcDHODH (molecular mass of ~34 kDa for the dimeric protein) found in the soluble fraction was loaded onto a 2-mL column of Ni–NTA resin equilibrated with lysis buffer (50 mM sodium phosphate [pH 8.0] and 300 mM NaCl). The column was then washed with a step gradient of imidazole from 0 to 100 mM in lysis buffer plus imidazole. The washes consisted of 40 mL of lysis buffer with no imidazole followed by 50 mL of lysis buffer plus 25 mM imidazole and then 10 mL of lysis buffer plus 50 mM imidazole. The recombinant TcDHODH was eluted with approximately 20 mL of lysis buffer in the presence of 100 mM imidazole, and purity was checked on 12% SDS–PAGE electrophoretic gels. Ultraviolet (UV) absorbance at 280 nm, based on tryptophan and tyrosine residue molar extinction coefficients, was used to estimate protein concentration [13]. The extinction coefficient calculated for the recombinant TcDHODH was 15,840 M^{-1} cm^{-1}. Active fractions were dialyzed at 4 °C against phosphate-buffered saline (50 mM sodium phosphate and 150 mM NaCl [pH 8.0]) and Tris-buffered saline (20 mM Tris and 150 mM NaCl [pH 8.0]). The enzyme was concentrated with 10 kDa Amicon (Millipore) in Tris-buffered saline.

Determination of apparent enthalpy of reaction

The apparent molar enthalpy (ΔH_{app}) of conversion of DHO to orotate by TcDHODH was determined by ITC as follows. The calorimeter sample cell, with 1.43 mL, was loaded with Tris-buffered saline (pH 8.0) containing 1.6 mM fumarate and 300 nM TcDHODH and was titrated by a single injection of 10 μL from a syringe loaded with 3.0 mM DHO in the same buffer. After a preliminary equilibration period, when the instrument reached the temperature of 298 K, an additional 60-s delay period was allowed to generate the baseline. After this delay, the reaction was automatically started by the injection of DHO with a heat reference at 25 μcal s^{-1}. The complete depletion of DHO and end of reaction were indicated by the return of the instrumental thermal power to the baseline. The stirring speed of the injection syringe was set to 307 rpm. Heat flow (microcalories per second) was recorded as a function of time. The heat generated by dilution of the substrate was determined under the same experimental conditions except for the absence of enzyme [14]. The apparent molar enthalpy was then determined by subtracting the heat of dilution from the total heat evolved during the reaction and dividing by the number of DHO moles injected into the sample cell. The heat involved in the assay was found by integrating the area under the heat flow curve. The heat from buffer ionization was checked by performing the apparent enthalpy experiment under the same conditions but with a different buffer, namely phosphate-buffered saline (pH 8.0).

Enzyme kinetics by ITC

Titration experiments were carried out with a VP-ITC calorimeter (MicroCal, Northampton, MA, USA) [15]. Solutions were de-

gassed by means of a vacuum degasser (ThermoVac, MicroCal) and thermostated for 5 min prior to any experimental run. A heating reference of 25 μcal s^{-1} was used in all experiments. The heat flow released during the enzyme-catalyzed reaction was measured and was found to be directly proportional to the rate of the reaction (V). The relationships shown in Eqs. (1)–(3) below allow the kinetic parameters maximal velocity, apparent catalytic constant, and Michaelis constant (V_{max}, k_{cat}^{app}, and K_M, respectively) to be determined from a single ITC experiment. Although the VP-ITC calorimeter employed in this work is not meant to be of use in high-throughput screening (HTS), the results outlined here will be useful for those who work in this very important area of enzyme inhibition. For HTS results used to identify lead candidates for drug development, an optimization algorithm based on enthalpic and entropic information generated by ITC was put forward recently [16]. On the other hand, it is noteworthy that using the new ITC_{200}, a throughput of up to 75 samples per day with a capacity to run 384 samples unattended is already at a hand.

$$V = \frac{d[P]_t}{dt} = \frac{1}{\Delta H_{app} V_0} \frac{dQ}{dt}, \tag{1}$$

where $[P]_t$ is the instantaneous product concentration, V_0 is the constant volume of the sample cell (1.43 mL), and dQ/dt is the rate of heat flow measured during the experiment. The apparent molar enthalpy (ΔH_{app}) of the conversion of substrate to product is determined experimentally (see above).

The substrate concentration $[S]_t$ is calculated at any time using the expression

$$[S]_t = [S]_0 - \frac{\int_0^t \frac{dQ}{dt} dt}{V_0 \Delta H_{app}}, \tag{2}$$

where $[S]_0$ is the initial substrate concentration.

The kinetic parameters V_{max} and K_M were obtained by fitting the calorimetric data to the Michaelis–Menten equation [17] (Eq. (3)) using nonlinear least squares regression analysis:

$$V = \frac{V_{max}[S]_t}{K_M + [S]_t}. \tag{3}$$

Because the TcDHODH enzymatic catalysis is dependent on the two substrates, DHO and fumarate, the assays were performed under pseudo-first-order conditions by using an excess of one substrate and titrating the other. To follow the kinetic behavior of DHO, a syringe was filled with the Tris-buffered saline (pH 8.0) containing 3.0 mM DHO and the sample cell was filled with the same buffer containing 1.6 mM fumarate and 50 nM TcDHODH enzyme. DHO was titrated by 20 injections of 1.0 μL. To analyze the second substrate, 15 injections of 3.0 μL of fumarate (16 mM in buffered solution) were titrated into the sample cell filled with 300 nM TcDHODH and 4 mM DHO in the same Tris-buffered saline. These experiments were carried out at 298 K and a stirring speed of 307 rpm.

Spectrophotometric method for determination of TcDHODH reaction

The TcDHODH reaction was conventionally assayed in the spectrophotometer in parallel to the ITC method with 50 nM TcDHODH, with the substrate DHO varying from 10 to 50 μM and fumarate in excess (1.6 mM). A second assay was carried out with fumarate at various concentrations ranging from 100 to 400 μM, DHO at 4 mM, and TcDHODH at 300 nM. The reaction was started by injecting enzyme into the reaction mixture in Tris-buffered saline (pH 8.0) at 25 °C (pH 8.0). Kinetic data were obtained by measuring the formation of the product orotate. The molar extinction coefficient for orotate at 300 nm used was 2650 M^{-1} cm^{-1}.

Kinetic parameters and apparent enthalpy in the presence of cosolvent and nonionic surfactant

TcDHODH enzyme activity was investigated in the presence of organic cosolvent DMSO and the nonionic surfactant Triton X-100. The isothermal titration experiments were carried out with 16 mM fumarate in the syringe and 300 nM TcDHODH and 4.0 mM DHO in the sample cell. All solutions were prepared in Tris-buffered saline (pH 8.0). The substrate was titrated by 15 injections of 3.0 μL into the sample cell in the presence of DMSO (10%, v/v) or Triton X-100 (0.5%, v/v) with an interval of 120 s between injections at 298 K. The reference power was 25 μcal s^{-1}, and the stirring speed was 307 rpm.

The molar apparent enthalpy (ΔH_{app}) of reaction was determined by filling the sample cell with 1.6 mM fumarate and 300 nM TcDHODH and filling the syringe with 3.0 mM DHO. The reaction was buffered in 20 mM Tris and 150 mM NaCl (pH 8.0) at a temperature of 298 K and was titrated by one injection of 10 μl in the presence of DMSO (10%, v/v) or Triton X-100 (0.5%, v/v) (heat reference: 25 μcal s^{-1}). Control experiments were carried out in the absence of any cosolvent.

Enzyme inhibition by orotate

In the calorimetric TcDHODH inhibition assay, the syringe was filled with 16 mM fumarate and the sample cell was filled with 4.0 mM DHO and 300 nM TcDHODH, with all solutions being prepared in Tris-buffered saline (pH 8.0). Fumarate was titrated by 15 injections of 3.0 μL at intervals of 120 s at a temperature of 298 K, reference power of 25 μcal s^{-1}, and stirring speed of 307 rpm. A control experiment was performed in the absence of orotate. To carry out the enzyme inhibition evaluation by orotate, it was added to the sample cell at varied concentrations of 50, 100, 200 and 300 μM.

Determination of thermodynamic reaction parameters of activation

The thermodynamic parameters of activation were carried out by multiple injection titrations of each substrate into an excess of the other in the presence of TcDHODH at 293, 298, 303, and 310 K. The ITC sample cell was filled with 1.6 mM fumarate and 50 nM TcDHODH enzyme, and 20 injections of 1.0 μL of DHO (3.0 mM) solution were added to protein solution in the ITC cell with 60-s interval monitoring and a stirring speed of 307 rpm.

The kinetic behavior of fumarate was then investigated by filling the syringe with the buffer solution containing 16 mM fumarate. The sample cell was filled with the buffered solution of 4.0 mM DHO and 300 nM TcDHODH. The experiments were carried out titrating the fumarate by 15 injections of 3.0 μL with an interval between injections of 120 s, a stirring speed of 307 rpm, and temperatures at 293, 298, 303, and 310 K. An initial delay period of 60 s was allowed to generate the baseline used in the subsequent data analyses. Heat flow (μcal s^{-1}) was recorded as a function of time.

To deduce the temperature dependence of the reaction, kinetic parameters were analyzed by making Arrhenius plots for temperatures ranging from 293 to 310 K. The activation energy (E_a) was calculated from the slope (E_a/R) of the Arrhenius plot, and then the thermodynamic activation parameters enthalpy ($\Delta H^{\#}$), entropy ($\Delta S^{\#}$), and Gibbs free energy ($\Delta G^{\#}$) of activation were estimated by the following equations [18]:

$$\Delta H^{\#} = E_a - RT, \tag{4}$$

$$\Delta G^{\#} = RT(\ln(k_B/h) + \ln T - \ln k_{cat}^{app}), \tag{5}$$

and

$$\Delta S^{\#} = (\Delta H^{\#} - \Delta G^{\#})/T, \tag{6}$$

where energy values are in kJ mol^{-1}, with k_{cat} in s^{-1}, to conform to the units of the Boltzmann (1.3805×10^{-23} J K^{-1}) and Planck (6.6256×10^{-34} J s^{-1}) constants and R is the gas constant (8.314 J mol^{-1} K^{-1}).

Data analysis

ITC raw data analyses of enthalpy of reaction were performed with the graphic analysis program Origin 7.0, and the data representing the heat dilution effects, due to substrate dilution into the buffer and mixing, were subtracted from the raw heat flow data [19]. Kinetic parameters were analyzed and calculated in the enzyme assay mode of the program SigmaPlot 10.0.

Results

Apparent enthalpy of TcDHODH reaction

In ITC reaction experiments, the amount of heat exchanged is proportional to the apparent molar enthalpy (ΔH_{app}). In this experiment, a large amount of enzyme was placed in the sample cell to ensure that all of the substrate was converted to product. DHO substrate was chosen as the limiting reactant. The injection of 10 μL led to a dilution of the DHO from 3.0 mM (syringe) to 21 μM (sample cell), whereas fumarate remained at a constant concentration of 1.6 mM in the sample cell (Fig. 1).

Fig. 1 shows a typical calorimetric trace (heat flow vs. time). The output signal adopts negative values because it represents the variation in the current feedback in the reference cell required to compensate the heat released by the reaction in the sample cell. The reaction goes to completion, allowing ΔH_{app} to be determined by integrating the total peak area in the calorimeter trace. ΔH_{app} was calculated with Eq. (7):

$$\Delta H_{app} = \frac{1}{[S]_{tot} V_0} \int_0^t \frac{dQ}{dt}. \quad (7)$$

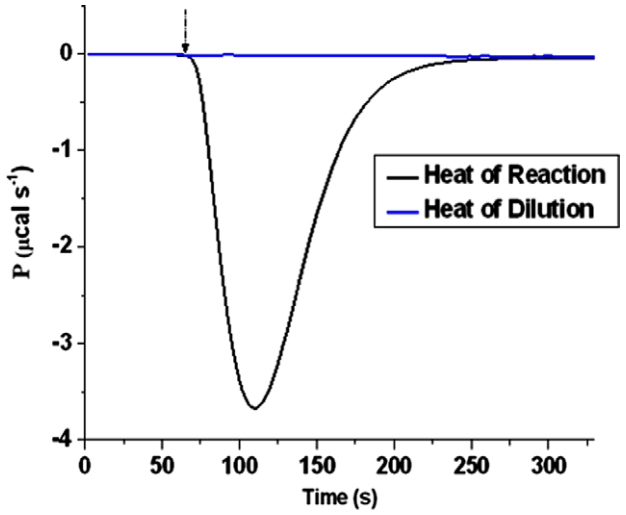

Fig. 1. Heat flow as a function of time (μcal s^{-1}) for the oxidation of DHO to orotate and the reduction of fumarate to succinate. The arrow corresponds to the substrate injection and reaction start. The temperature was set to 298 K, and the instrument thermal power was monitored until baseline return to initial value. DHO (3.0 mM) in the syringe was titrated in a single injection of 10 μl into the sample cell containing 1.6 mM fumarate and 300 nM TcDHODH. Buffer: 20 mM Tris and 150 mM NaCl (pH 8.0). The blue curve is the heat of substrate dilution under the same conditions in the absence of TcDHODH. Reaction heat was subtracted from the dilution event. (For interpretation of the reference to color in this figure legend, the reader is referred to the Web version of this article.)

The ΔH_{app} obtained was −11.64 ± 1.78 kcal mol^{-1} (from three independent measurements). This ΔH_{app} value was used to calculate the reaction rate (Eq. (1)) as described below.

Calorimetric determination of TcDHODH enzyme activity

The reaction rate depends on both fumarate and DHO concentrations, but it is describable in terms of pseudo-first-order kinetics when one of them is maintained in excess [14]. The enzyme activity was monitored for both substrates in separate experiments at different concentrations. Initially, optimal concentrations of the enzyme and substrate were determined by monitoring the conversion of fumarate to succinate by TcDHODH via ITC. One requirement for an enzyme to operate via the Michaelis–Menten mechanism is fulfilled when it reaches the steady-state condition, where the concentration of the enzyme–substrate complex [*ES*] remains constant at a given substrate concentration. Fig. 2 shows raw data for thermal power plotted against time in the multiple injection assays.

Steady-state conditions were verified in two different ways. The first way was to analyze the plateaus established between the injections, where the concentration of intermediate [*ES*] remains constant, when the rates of formation and breakdown of the complex were equal. As a result, a well-defined plateau was observed, as shown in the inset of Fig. 2. The second way was to design an experiment in which the amount of substrate was altered during the time course of the reaction by injecting different volumes of substrate (Fig. 3). If the reaction proceeds under steady-state conditions, the kinetic parameters do not change. Kinetic parameters are summarized in Table 1.

Fig. 4A shows the reaction rate dependence on DHO concentration, and Fig. 4B shows the reaction rate dependence on fumarate concentration.

The kinetics of the DHOD-catalyzed enzyme reaction was explored by both UV–visible spectrophotometry and ITC. The two experiments were carried out with the same solutions and enzyme aliquots to minimize the differences due to operational errors and variations in enzyme activity. The kinetic parameters determined are of the same order of magnitude as those reported for the DHOD family (Table 2).

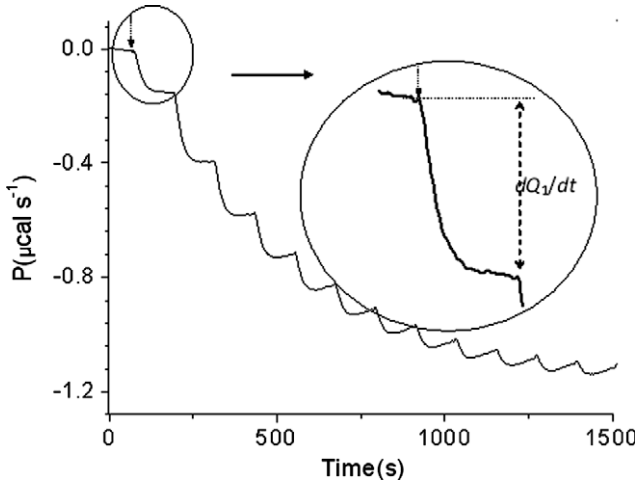

Fig. 2. ITC raw data for change in thermal power over time in the multiple injection assay. As can be seen, dQ_1/dt (heat flow) is proportional to the heat released in the sample cell. Under the conditions used, a steady state is reached when enzyme velocity (power) remains constant. The arrow corresponds to the first injection of substrate into the sample cell. The experiment was performed at 298 K in Tris-buffered saline, with 15 injections of 3.0 μL of 16 mM fumarate being titrated into the sample cell filled with 300 nM TcDHODH and 4.0 mM DHO.

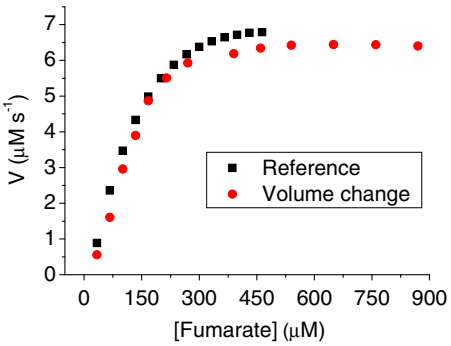

Fig. 3. Experimental verification of steady state in reaction rate data. Red curve: varying substrate volumes injected (5 injections of 3 μl and 3 injections each of 5, 7, and 10 μL of 16 mM fumarate titrated into the sample cell filled with 300 nM TcDHODH and 4 mM DHO in Tris-buffered saline (pH 8.0) at 298 K. Reference: 15 injections of 3 μL of 16 mM fumarate titrated into the sample cell filled with 300 nM TcDHODH and 4 mM DHO in Tris-buffered solution (pH 8.0). Velocity was adjusted to a Michaelis–Menten equation. (For interpretation of the reference to color in this figure legend, the reader is referred to the Web version of this article.)

Table 1
Kinetic parameters of steady-state experiment verification.

	K_M (μM)	V_{max} (μM s^{-1})
Reference	120 ± 9	6.71 ± 0.15
Volume change	118 ± 3	6.42 ± 0.12

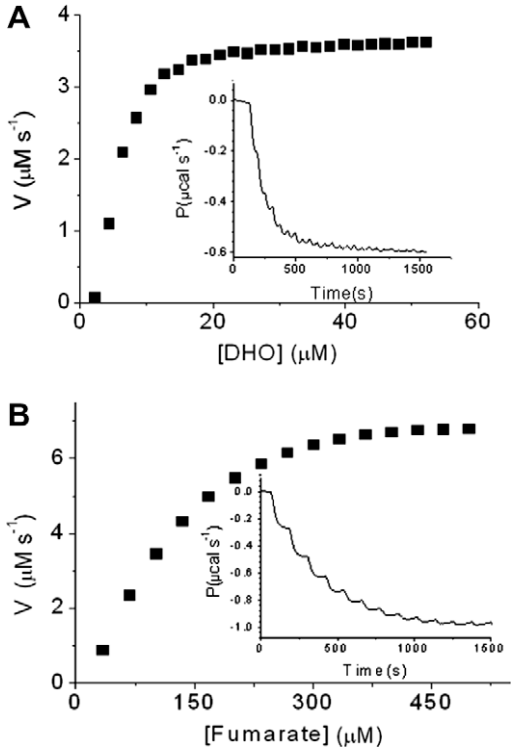

Fig. 4. Nonlinear least squares analyses of the experimental data to the Michaelis–Menten equation to determine the kinetic parameters. The inset panel shows ITC raw data for rate of heat flow plotted against time in the multiple injection titrations. (A) Total of 20 injections of 1.0 μL of 4.0 mM DHO into the sample cell containing 16 mM fumarate and 50 nM TcDHODH (pH 8.0) at 298 K. K_M = 8.56 ± 2.6 μM. (B) Total of 15 injections of 3.0 μL of 16 mM fumarate titrated into the sample cell filled with 300 nM TcDHODH and 4.0 mM DHO. Under these conditions, product inhibition was thoroughly avoided. K_M = 120 ± 9.0 μM.

Table 2
Comparison of K_M values of family 1A of DHODs.

Species	DHO (μM)	Fumarate (μM)	Method
Recombinant *Trypanosoma cruzi* (Y strain)	8.56 ± 2.6	120 ± 9.0	ITC
	12.9 ± 5.4	147 ± 17	UV
Leishmania major Friedlin[a]	57.9	143	UV
Trypanosoma brucei[b]	14.0	80.0	UV
Lactococcus lactis[c]	35.0 ± 2.0	ND	UV
Saccharomyces cerevisiae[d]	16.0 ± 5.0	115 ± 5.0	UV

Note. ND, not determined.

[a] The orotate production was measured spectrophotometrically at 300 nm (ε = 2.65 mM^{-1} cm^{-1}) in a reaction mixture containing 50 mM Tris (pH 8.0) and 150 mM KCl with the substrates DHO and fumarate in a total volume of 1.0 mL at 25 °C [20].

[b] Assays were performed in buffer (50 mM Hepes [pH 8.0], 150 mM NaCl, and 10% glycerol) at 25 °C in the presence of 500 mM fumarate, and fumarate-dependent activity was assayed in the presence of 250 mM DHO [21].

[c] Determined from orotate production by measuring absorption at various wavelengths in 0.1 M potassium phosphate (pH 7.5) at 37 °C [22].

[d] 1.0 mM DHO as substrate and 1.0 mM fumarate in 50 mM Tris–HCl, 150 mM KCl, and 0.1% (v/v) Triton X-100 (pH 8.0) at 30 °C by monitoring the increase in UV absorption of the product orotate [23].

Determination of enzyme activity in the presence of DMSO and Triton X-100

The activity of TcDHODH was observed in the presence of DMSO and the surfactant Triton X-100. Table 3 summarizes the molar enthalpy (ΔH_{app}), Michaelis–Menten constant (K_M), maximum velocity (V_{max}), and catalytic efficiency (k_{cat}^{app}/K_M) with fumarate controlling the biochemical reaction.

Effect of orotate on TcDHODH reaction

The effect of product concentration on reaction medium was assessed by determining the apparent inhibition constant (K_i^{app}) from Fig. 5A. The rate of reaction (V) was measured at various concentrations of orotate in the sample cell. The Lineweaver–Burk double reciprocal plot is shown in Fig. 5B. The (K_i^{app} obtained by nonlinear least squares regression fitted the experimental data to the model for competitive inhibition, Eq. (8), using SigmaPlot 10.0 software:

$$V = \frac{V_{max}[S]}{[S] + K_M\left(1 + \frac{[I]}{K_i}\right)}, \tag{8}$$

where [I] is the inhibitor concentration.

The value of V_{max} is constant at all inhibitor concentrations, but the apparent value of K_M (taken to be (1 + [I]/K_i)) increases with inhibitor concentration. The effects are most apparent in the

Table 3
Molar enthalpy, Michaelis–Menten constant, maximal velocity, and catalytic efficiency for fumarate-limited catalyzed reaction in the presence of DMSO and Triton X-100.

Parameter[a]	Control	10.0% (v/v) DMSO	0.5 % (v/v) Triton X-100
ΔH_{app}[b] (kcal mol^{-1})	−11.64 ± 0.49	−10.73 ± 0.37	−10.81 ± 0.30
k_{cat}^{app} (s^{-1})	20.5	16.5	13.6
V_{max} (μM s^{-1})	6.16 ± 0.15	4.94 ± 0.10	4.04 ± 0.24
K_M (μM)	120.00 ± 9.00	110.00 ± 7.39	84.70 ± 9.32
k_{cat}^{app}/K_M 10^3(M^{-1} s^{-1})	171	150	160

[a] Kinetic parameter for TcDHODH (EC 1.3.99.11) enzyme determined as shown in Fig. 4B for the substrate fumarate.

[b] The molar enthalpy values were determined separately, with typical ΔH values for small molecule association to proteins in the range of 1–25 kcal mol^{-1} depending on the experimental conditions [24].

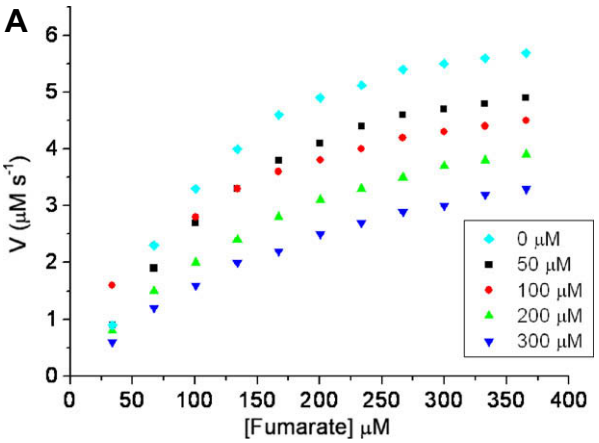

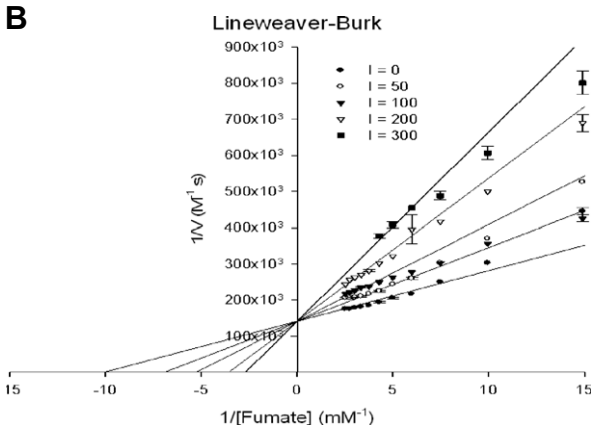

Parameters					
Value		±Standard Error	95% Conf. Interval		
V_{max} (μM s^{-1})	7.06	1.39	6.78	to	7.33
K_M (μM)	120.05	7.42	109.12	to	130.0
K_i (μM)	109.83	6.63	96.69	to	122.98
Goodness of Fit					
Degrees of Freedom	107				
AICc	-2.879.92				
R^2	0.97				
Sum of Squares	$4.35x10^{-10}$				
Sy.x	$2.02 x10^{-10}$				
Runs Test p Value	< .001				

Fig. 5. Calorimetric TcDHODH assay in the presence of orotate. (A) Control experiment: 16 mM fumarate in the syringe, 4.0 mM DHO, and 300 nM TcDHODH in the sample cell. All solutions were made up in Tris-buffered solution (pH 8.0), with fumarate titrated by 11 injections of 3.0 μL at intervals of 120 s and 298 K. The reference power was 25 μcal s^{-1}, and the stirring speed was 307 rpm. Inhibition experiment: in the sample cell, 50 μM orotate. (B) Double reciprocal plots obtained at various orotate concentrations: 0 (control), 50, 100, 200, and 300 μM. A competitive nonlinear model was fitted to data in the SigmaPlot program with (K_i^{app} = 110 ± 6.6 μM (from two independent measurements). The (K_i^{app} dimeric fit is performed considering the total protein concentration as obtained by the method of molar extinction coefficient.

double reciprocal plot (Fig. 5B), where the $1/V_{max}$ intercept is constant for all lines but their slopes (K_M/V_{max}) and x-intercept ($-1/K_M$) vary with inhibitor concentration.

Determination of thermodynamic parameters of activation

The activation energies of the TcDHODH reactions were calculated by determining the slope ($-E_a/R$) of the Arrhenius plots, and the thermodynamic activation parameters at 298 K were estimated from Eqs. (4)–(6) and are summarized in Table 4.

Modus operandi and control

The reaction began after the substrate injection, and the ITC baseline then registered a negative deflection (Fig. 1), typical of an exothermic reaction. A control experiment was done under

Table 4
Thermodynamic activation parameters for the reaction catalyzed by TcDHODH at 298 K.

Parameter	Fumarate	DHO
k_{cat}^{app} [a]	20.5 ± 1.6	45.0 ± 1.4
$\Delta G^{\#}$ (kcal mol^{-1})	15.6 ± 0.1	15.2 ± 0.1
$\Delta\Delta G^{\#}$ [b]	0.4	0
E_a (kcal mol^{-1})	6.0 ± 0.3	3.0 ± 0.8
ΔE_a	3.0	0
$\Delta H^{\#}$ (kcal mol^{-1})	5.5 ± 0.2	2.4 ± 0.8
$\Delta\Delta H^{\#}$	3.1	0
$-T\Delta S^{\#}$ (kcal mol^{-1})	10.1 ± 0.2	12.8 ± 0.1
$-T\Delta\Delta S^{\#}$	−2.7	0

[a] k_{cat}^{app} is given in s^{-1}.
[b] $\Delta\Delta G^{\#}$, ΔE_a, $\Delta\Delta H^{\#}$, and $-T\Delta\Delta S^{\#}$ represent the differences between each pair of values: $TcDHODH_{fumarate} - TcDHODH_{DHO}$.

the same reaction conditions but in the absence of enzyme to allow the determination of the heat of dilution of the injected substrate shown in the blue curve. The area above the peak of the black line corresponds to the total heat (Q_T) released in the reaction. Solutions in the syringe and in the sample cell were prepared in the same buffer, pH, and salt concentration to minimize heat associated with dilution, diffusion, and mixture of solutions.

The reaction reached a maximum heat release at around 120 s, after which the signal gradually returned to the baseline. The total depletion of limiting substrate took place at around 250 s, indicating the end of the reaction. The reaction heat was subtracted from the dilution event (blue curve) and yielded $\Delta H_{app} = -11.64 \pm 1.78$ kcal mol^{-1} (three independent measurements). The buffer proton exchange heat was checked by performing the same measure runs in 50 mM sodium phosphate buffer, and no changes in ΔH_{app} were observed (data not shown), suggesting as expected that there was no proton exchange with the buffer.

One requirement for an enzyme to operate through a Michaelis–Menten mechanism is that the steady-state condition should be reached, where the concentration of the enzyme–substrate complex [*ES*] remains constant at a given substrate concentration. After the first injection of fumarate, the reaction starts (Fig. 2 shows the raw data) and the baseline decreases from the initial level to a lower plateau that corresponds to the heat flow according to the reaction rate. The difference between the two plateaus is related to the velocity at a given substrate concentration (dQ/dt) [19]. Each injection increases the amount of limiting substrate in the sample cell, so that the reaction rate increases and the baseline assumes a new plateau at a lower level until enzyme saturation takes place and the reaction velocity reaches its maximum.

Discussion

As can be seen in Fig. 3, the reaction catalyzed by TcDHODH enzyme is in the steady-state condition. Multiple injections of various volumes, and consequently different concentrations of substrate injected into the sample cell, did not alter the kinetic parameters determined. A behavioral performance of TcDHODH reaction with 3 μL of fumarate injected into the sample cell was observed (Table 1 and Fig. 3).

In Fig. 4A, to ensure a pseudo-first-order reaction curve in relation to the substrate DHO, fumarate was present in excess, whereas in Fig. 4B, the reaction curve is pseudo-first order in relation to the substrate fumarate.

DHO and fumarate had their Michaelis constants calculated by fitting the experimental velocity in the Michaelis–Menten equation, and their K_M values were 8.6 ± 2.6 and 120 ± 9.0 μM, respectively. Thus, DHO binds effectively to the enzyme active site at a much lower concentration than fumarate, according to its small K_M value. Maximum velocities (V_{max}) were calculated to be 4.1 ± 0.7 μM s^{-1} for DHO and 6.7 ± 0.1 μM s^{-1} for fumarate, but DHO requires 14-fold lower concentration than fumarate to achieve the V_{max}.

Data in Table 2 are consistent with previous attempts to compare ITC and established spectroscopic assays [25]. Analyzing the UV and ITC methods in determining the Michaelis–Menten constant, we observed ratios of 1.51 for the substrate DHO and 1.23 for the substrate fumarate. In this case, the kinetic parameters by ITC and UV–visible spectroscopy agree well. Nevertheless, when a difference occurs, we can infer that ITC can reveal parallel reactions not detected by conventional assays [18].

The value of K_M depends on the substrate and on environmental conditions such as pH, temperature, ionic strength, and polarity, and it provides a measure of the substrate concentration required for significant catalysis to occur.

Comparisons between methods and the kinetic parameters of the 1A family of DHOD must be made carefully because experimental conditions differ widely in terms of pH, buffer, substrate concentration, and temperature [26]. High-quality kinetic data are obtained by ITC because the rate of reaction is detected directly and multiple injections of substrate are made automatically; furthermore, ITC measurements do not depend on optical methods. Kinetic parameters measured by microcalorimetry are accurate and precise.

In this study, we also exposed the TcDHODH enzyme to DMSO (10%, v/v) and Triton X-100 (0.5%, v/v) (Table 3), and as expected, they did not affect the enthalpies of reaction. However, the maximum velocities using these concentrations along with all defined concentrations described in Materials and methods decreased to 80% in DMSO and to 66% in Triton X-100 when compared with the control experiments. Both of them increase the hydrophobicity of the solution, and this seems to facilitate the substrate binding process; on the other hand, the catalytic efficiency decreases. At lower K_M values, the TcDHODH enzyme is more easily saturable and, therefore, has a low V_{max}.

After the establishment of a protocol to study the enzyme kinetics by the ITC method, the product of the reaction TcDHODH, a known inhibitor of the enzyme, was investigated by a new *modus operandi*. The full enzymatic activity curve allowed the determination of the apparent inhibition constant ($K_i^{app} = 110$ μM ± 6.6) as well as the mechanism of inhibition in relation to the substrate fumarate, both of which are essential in studies of structure–activity relationships. The Lineweaver–Burk method was used to derive the inhibition constant for orotate. The curve showed the best fit to the data in the competitive inhibition model ($R^2 = 0.97$). Thus, orotate competes for the same active site on the enzyme as the substrates DHO and fumarate, and the formation of an enzyme–inhibitor complex is possible. Thus, orotate can be used as a control standard inhibitor during the screening of new compounds against TcDHODH.

Knowledge of the enzyme–substrate transition structure provides fundamental information on the interactions occurring in the reaction and provides a blueprint for the design of transition state structure-based inhibitors [27].

In Fig. 6, we show a brief description of the transition state structure based on the information in the literature, where flavin mononucleotide (FMN) is the prosthetic group [28,29].

The catalytic residue Cys130 withdraws a proton from DHO while a hydride is transferred to FMN. In this step, the DHO is oxidized to orotate and the FMN_{ox} is reduced to FMN_{red}. The orotate is then released from the active site and the fumarate occupies its place. FMN transfers the hydride to fumarate, converting it in succinate while a proton is simultaneously abstracted from the Cys130 catalytic group, reestablishing the enzyme for a new catalytic cycle.

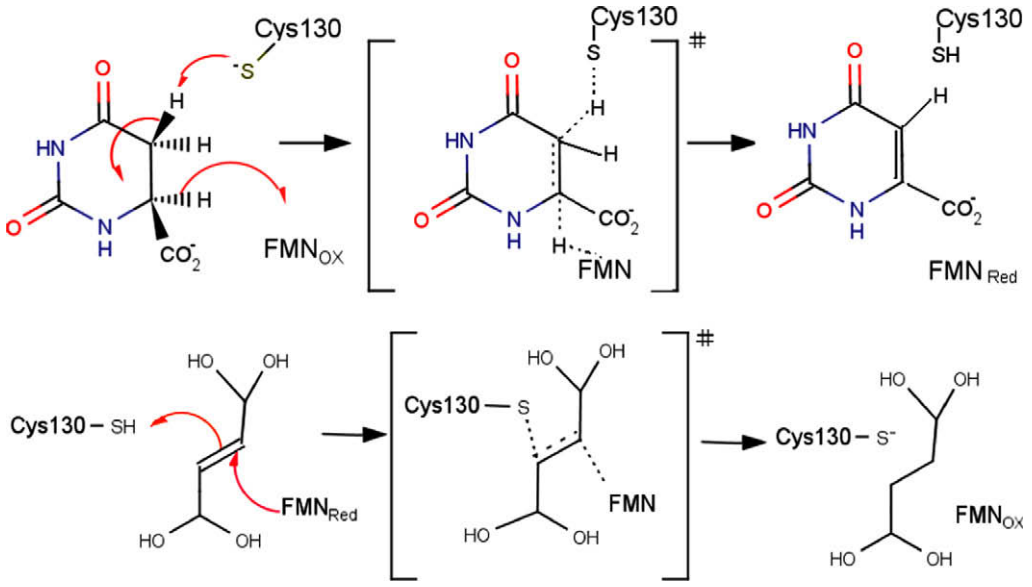

Fig. 6. Catalytic mechanism illustrated to TcDHODH enzyme. First half-reaction: DHO oxidation via single transition state in which the active site has a Cys and a proton is transferred to the flavin cofactor. Second half-reaction: fumarate reduction.

Thermodynamic parameters of this process were thoroughly measured in this study. They are related to the differences between the ground state (*ES*) and the activated enzyme–substrate complex ($ES^{\#}$) for a hypothetical equilibrium, where the reagents only follow through this state. It is important to recollect that the transition state theory contains several simplifications in describing a complex phenomenon such as an enzymatic reaction, but the thermodynamic parameters derived from this description are helpful in dissecting structure–reactivity relationships in the search for transition state inhibitor analogs.

The values of $\Delta G^{\#}$ represent the energy barrier required for reactions to occur. The $\Delta\Delta G^{\#}$ value (Table 4) reveals the difference of k_{cat}^{app} between the TcDHODH pseudo-first-order catalyses of fumarate and DHO. $\Delta G^{\#}$ is higher for the reduction of fumarate than for the oxidation of DHO by 0.40 kcal mol^{-1}, implying that fumarate reduction is the rate-limiting step of the reaction catalyzed by TcDHODH.

In the range of temperatures studied, no significant variations in $\Delta G^{\#}$ was observed, suggesting a similar overall process in the formation of the active complex between enzyme and substrates. $\Delta H^{\#}$ is of

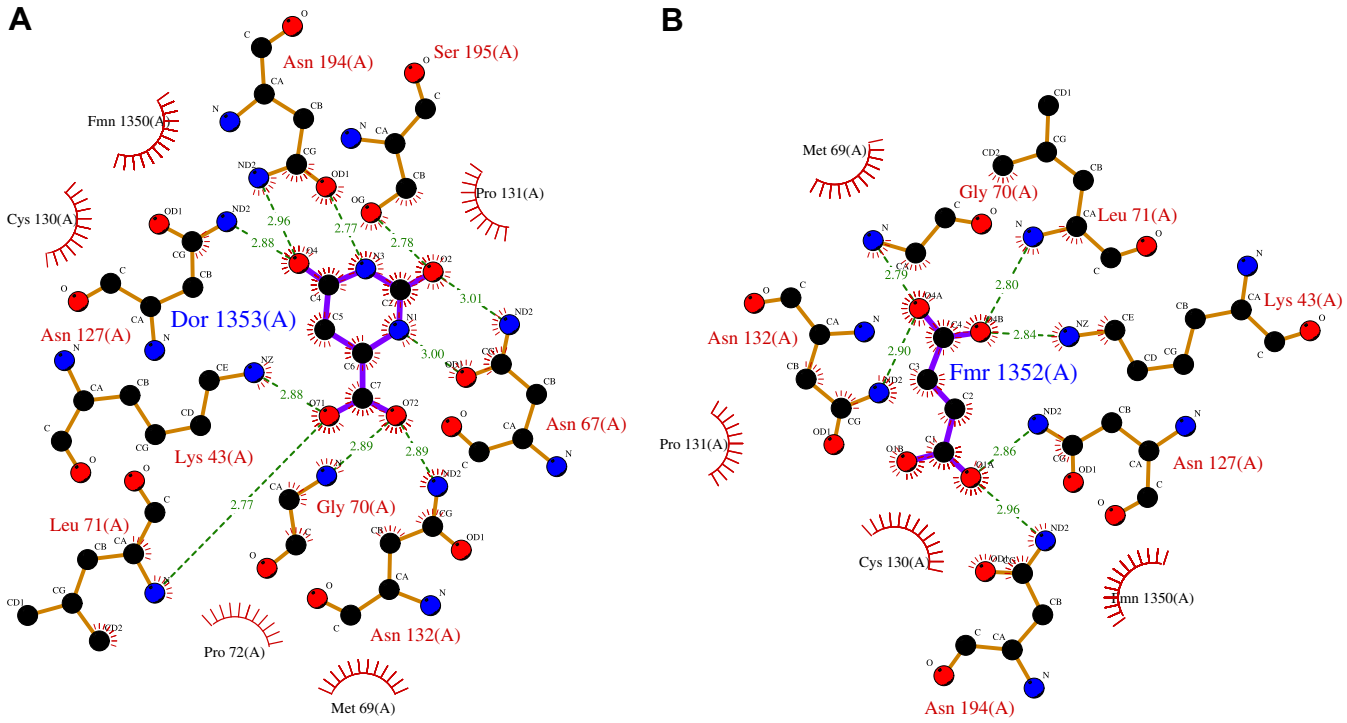

Fig. 7. Map of interactions between TcDHODH enzyme active site and substrates DHO and fumarate. Donor/Acceptor hydrogen patterns in agreement with calorimetric results: the enzyme–DHO complex (A) has 10, whereas the enzyme–fumarate complex (B) has 6. Figures are taken from the PDB Sum databank with codes 2e68 and 2e6d (http://www.ebi.ac.uk/pdbsum/2e68 and http://www.ebi.ac.uk/pdbsum/2e6d, respectively).

the same order of magnitude as most reported values [30], and $\Delta S^{\#}$ has the major contribution to the $\Delta G^{\#}$ for both substrates. Activation enthalpy is 1.8- and 5.3-fold less effective than the entropic energy barriers of fumarate and DHO, respectively; the latter (>10 kcal · mol^{-1}) contributes unfavorably to the transition state.

To understand the enthalpy parameter, an analysis of the process can be made in two different steps. The first step is the binding event between substrate and enzyme, which is favorable and has a negative enthalpy (Table 3), and the second step is the formation of the transition state. Comparative analyses of cocrystal structures for the two substrates (PDB codes: 2e68 and 2e6d) show more complementary interactions in the DHO–enzyme complex than in the fumarate–enzyme complex (Fig. 7).

The fact that fumarate and DHO target the same active site allows the two complex structures to be compared and correlated with the thermodynamic activation parameters determined by ITC. Fumarate has a more unfavorable activation enthalpy than DHO ($\Delta\Delta H^{\#}$ = 3.1 kcal mol^{-1}), and this difference may be attributed to the smaller number of hydrogen bonds found; the enzyme–DHO complex has 10, whereas the enzyme–fumarate complex has 6 (Fig. 7). Namely, the increase of rigidity of the hydrogen-bonding pattern favors the enzyme–DHO complex stabilization more than the enzyme–fumarate complex, and our energetics data capture this properly. According to the structure-based thermodynamic analysis, most of the enthalpically favorable interactions are due to polar interactions established by Lys, Asn, and Ser. The greater number of hydrogen interactions reflects favorably in the binding enthalpic contribution for the formation of the active complex when compared with the formation of the fumarate–enzyme complex.

Unfavorable entropy might be associated with a decrease in flexibility of the system, loss of rotation, and translation of the substrate molecule in the active complex. Another factor that might contribute to the large unfavorable entropy is the accessibility of each substrate to the TcDHODH active site; there is a loop at the entrance to the active site located over the FMN cofactor on the C-terminal end of the β-barrel that opens and closes the access channel of the substrate to the active site [28]. During the binding process of the formation of the DHO–enzyme active complex, there is a significantly greater loss of amino acid chain flexibility relative to the formation of the enzyme and the fumarate–enzyme active complex, reflecting the more unfavorable entropic value.

Enzyme conformations are related to each molecule to occupy an ensemble of conformation states. A change in temperature alters the number of conformation states occupied by enzymes, directly interfering in the binding (substrate–enzyme) events. Increasing the temperature, and consequently the number of conformation states occupied by enzymes, seems to lead to a decrease in substrate affinity.

An increase of temperature allows an increase in the number conformational states available to the enzyme TcDHODH. Higher enzyme conformation mobility will lead to a large proportion of enzyme molecules that will not bind to the substrate or will bind poorly; consequently, it leads to an increase in K_M values. This analysis agrees with the high unfavorable entropic contribution for $\Delta G^{\#}$ [31].

Conclusions

A customized biochemical assay protocol based on ITC has been employed for kinetic characterization of the TcDHODH enzyme reaction. These experiments demonstrated that ITC can be reliably used to monitor reactions of this type routinely, easily, and accurately with substrates and inhibitors that do not possess any spectroscopic probes. Other attractive features of the method are the ease and speed of the experiments. Enzyme assays are often laborious and time-consuming. The ITC method clearly detects the substrate saturation phenomenon and can easily record the enzyme activity in the steady state. If false positives are a problem in bioassays, cosolvent DMSO and nonionic surfactant Triton X-100 can be used to increase the solubility of small molecule ligands and avoid the aggregation of molecules. The method described in this article can allow the screening of compounds as potential *T. cruzi* DHOD inhibitors that could be used in Chagas disease chemotherapy. The product of the reaction, orotate, was found to inhibit the TcDHODH enzyme at high concentration in the mid-micromolar range and can be defined as a standard inhibitor for bioassays.

This study demonstrated that thermodynamic parameters improve our understanding of enzymatic mechanisms. Beside this, the transition state model elucidated by the calorimetric determination of thermodynamic data reported here can help us to evaluate the transition state of the reaction catalyzed by TcDHODH, and this may orientate future research on the design of transition state analogs.

Acknowledgment

We are grateful to the Fundação de Amparo à Pesquisa do Estado de São Paulo (FAPESP) and the Conselho Nacional de Pesquisa (CNPq) for financial support.

References

[1] C.M. Morel, J.R. Carvalheiro, C.N.P. Romero, E.A. Costa, P.M. Buss, The road to recovery, Nature 449 (2007) 180–182.
[2] C.J. Schofield, J. Jannin, R. Salvatella, The future of Chagas disease control, Trends Parasitol. 22 (2006) 583–588.
[3] E. Zameitat, G. Freymark, C.D. Dietz, M. Loffler, M. Bolker, Functional expression of human dihydroorotate dehydrogenase (DHODH) in pyr4 mutants of *Ustilago maydis* allows target validation of DHODH inhibitors in vivo, Appl. Environ. Microb. 73 (2007) 3371–3379.
[4] T. Nara, T. Hshimoto, T. Aoki, Evolutionary implications of the mosaic pyrimidine-biosynthetic pathway in eukaryotes, Gene 257 (2000) 209–222.
[5] S.G. Couto, M. Cristina Nonato, A.J. Costa-Filho, Defects in vesicle core induced by *Escherichia coli* dihydroorotate dehydrogenase, Biophys. J. 94 (2008) 1746–1753.
[6] T. Annoura, T. Nara, T. Makiuchi, T. Hashimoto, T. Aoki, The origin of dihydroorotate dehydrogenase genes of kinetoplastids, with special reference to their biological significance and adaptation to anaerobic, parasitic conditions, J. Mol. Evol. 60 (2005) 113–127.
[7] J.P. Overington, B. Al-Lazikani, A.L. Hopkins, How many drug targets are there?, Nat Rev. Drug Discov. 5 (2006) 993–996.
[8] H.J. Wiggers, J. Cheleski, A. Zottis, G. Oliva, A.D. Andricopulo, C.A. Montanari, Effects of organic solvents on the enzyme activity of *Trypanosoma cruzi* glyceraldehydes-3-phosphate dehydrogenase in calorimetric assays, Anal. Biochem. 370 (2007) 107–114.
[9] S.N. Olsen, Applications of isothermal titration calorimetry to measure enzyme kinetics and activity in complex solutions, Thermochim. Acta 448 (2006) 12–18.
[10] M.J. Todd, J. Gomez, Enzyme kinetics determined using calorimetry: a general assay for enzyme activity?, Anal Biochem. 296 (2001) 179–187.
[11] L. Di, E.H. Kerns, Biological assay challenges from compound solubility: strategies for bioassay optimization, Drug Discov. Today 11 (2009) 446–451.
[12] M.P. Pinheiro, J. Iulek, C.M. Nonato, Crystal structure of *Trypanosoma cruzi* dihydroorotate dehydrogenase from Y strain, Biochem. Biophys. Res. Commun. 369 (2008) 812–817.
[13] C.N. Pace, F.X. Schmidt, How to determine the molar absorbance coefficient of a protein, in: T.E. Creighton (Ed.), Protein Structure: A Practical Approach, second ed., IRL Press, New York, 1997, pp. 253–259.
[14] M.L. Bianconi, Calorimetric determination of thermodynamic parameters of reaction reveals different enthalpic compensations of the yeast hexokinase isozymes, J. Biol. Chem. 278 (2003) 18709–18713.
[15] T. Wiseman, S. Williston, J.F. Brandts, L.-N. Lin, Rapid measurement of binding constants and heats of binding using a new titration calorimeter, Anal. Biochem. 179 (1989) 131–137.
[16] E. Freire, A thermodynamic approach to the affinity optimization of drug candidates, Chem. Biol. Drug Des. 74 (2009) 468–472.
[17] L. Michaelis, M.L. Menten, Kinetics of invertase action, Kinetics of invertase action 49 (1913) 333–369.
[18] T. Lonhienne, E. Baise, G. Feller, V. Bouriotis, C. Gerday, Enzyme activity determination on macromolecular substrates by isothermal titration calorimetry: application to mesophilic and psychrophilic chitinases, Biochem. Biophys. Acta Prot. Struct. Mol. Enzymol. 1545 (2001) 349–356.

[19] MicroCal, ITC Data Analysis in Origin: Tutorial Guide, Version 7.0, MicroCal, Northampton, MA, 2004.
[20] P.R. Feliciano, A.T. Cordeiro, A.J. Costa-Filho, M.C. Nonato, Cloning, expression, purification, and characterization of *Leishmania* major dihydroorotate dehydrogenase, Protein Expr. Purif. 48 (2006) 98–103.
[21] T.L. Arakaki, F.S. Buckner, J.R. Gillespie, N.A. Malmquist, M.A. Phillips, O. Kalyuzhniy, J.R. Luft, G.T. DeTitta, C.L.M. Verlinde, W.C. Van Voorhis, W.G.J. Hol, E.A. Merritt, Characterization of *Trypanosoma brucei* dihydroorotate dehydrogenase as a possible drug target: structural, kinetic, and RNAi studies, Mol. Microbiol. 68 (2008) 37–50.
[22] F.S. Nielsen, P. Rowland, S. Larsen, K.F. Jensen, Purification and of dihydroorotate dehydrogenase A from *Lactococcus lactis*, crystallization, and preliminary X-ray diffraction studies of the enzyme, Protein Sci. 5 (1996) 852–856.
[23] E. Zameitat, A.J. Pierik, K. Zocher, M. Loffler, Dihydroorotate dehydrogenase from *Saccharomyces cerevisiae:* spectroscopic investigations with the recombinant enzyme throw light on catalytic properties and metabolism of fumarate analogues, FEMS Yeast Res. 7 (2007) 897–904.
[24] E. Poduch, A.M. Bello, S. Tang, M. Fujihashi, E.F. Pai, L.P. Kotra, Design of inhibitors of orotidine monophosphate decarboxylase using bioisosteric replacement and determination of inhibition kinetics, J. Med. Chem. 49 (2006) 4937–4945.
[25] D. Ajloo, A.A. Saboury, N. Haghi-Asli, G. Ataei-Jafarai, A.A. Moosavi-Movahedi, M. Ahmadi, K. Mahnam, S. Namaki, Kinetic, thermodynamic, and statistical studies on the inhibition of adenosine deaminase by aspirin and diclofenac, J. Enz. Inhib. Med. Chem. 22 (2007) 395–406.
[26] I. Schomburg, A. Chang, C. Ebeling, M. Gremse, C. Heldt, G. Huhn, D. Schomburg, BRENDA, the enzyme database: updates and major new developments, Nucleic Acids Res. 32 (2004) D431–D433.
[27] R.W. Miles, P.C. Tyler, R.H. Furneaux, C.K. Bagdassarian, V.L. Schramm, One-third-the-sites transition-state inhibitors for purine nucleoside phosphorylase, Biochemistry 37 (1998) 8615–8621.
[28] D.K. Inaoka, K. Sakamoto, H. Shimizu, T. Shiba, G. Kurisu, T. Nara, T. Aoki, K. Kiyoshi Kita, S. Harada, Structures of *Trypanosoma cruzi* dihydroorotate dehydrogenase complexed with substrates and products: atomic resolution insights into mechanisms of dihydroorotate oxidation and fumarate reduction, Biochemistry 47 (2008) 10881–10891.
[29] R.L. Fagan, K.F. Jensen, O. Bjornberg, B.A. Palfey, Mechanism of flavin reduction in the class 1A dihydroorotate dehydrogenase from *Lactococcus lactis*, Biochemistry 46 (2007) 4028–4036.
[30] M.R. Eftink, R.L. Biltonen, Energetics of ribonuclease A catalysis: III. Temperature dependence of the hydrolysis of cytidine cyclic 2′,3′-phosphate, Biochemistry 22 (1983) 5140–5150.
[31] T. Lonhienne, E. Baise, G. Feller, V. Bouriotis, C. Gerday, Enzyme activity determination on macromolecular substrates by isothermal titration calorimetry: application to mesophilic and psychrophilic chitinases, Biochim. Biophys. Acta 1545 (2001) 349–356.